Mon. Not. R. Astron. Soc. **000**, 1–10 (2008) Printed 4 November 2008 (MN LATEX style file v2.2)

The effect of photo-ionization on the cooling rates of enriched, astrophysical plasmas

Robert P.C. Wiersma,[1⋆] Joop Schaye[1] and Britton D. Smith[2]
[1] *Leiden Observatory, Leiden University, P.O. Box 9513, 2300 RA Leiden, The Netherlands*
[2] *Center for Astrophysics & Space Astronomy, Department of Astrophysical & Planetary Sciences, University of Colorado, Boulder, CO, 80309, USA*

arXiv:0807.3748v2 [astro-ph] 4 Nov 2008

4 November 2008

ABSTRACT

Radiative cooling is central to a wide range of astrophysical problems. Despite its importance, cooling rates are generally computed using very restrictive assumptions, such as collisional ionization equilibrium and solar relative abundances. We simultaneously relax both assumptions and investigate the effects of photo-ionization of heavy elements by the meta-galactic UV/X-ray background and of variations in relative abundances on the cooling rates of optically thin gas in ionization equilibrium. We find that photo-ionization by the meta-galactic background radiation reduces the net cooling rates by up to an order of magnitude for gas densities and temperatures typical of the shock-heated intergalactic medium and proto-galaxies ($10^4\,\mathrm{K} \lesssim T \lesssim 10^6\,\mathrm{K}$, $\rho/\langle\rho\rangle \lesssim 100$). In addition, photo-ionization changes the relative contributions of different elements to the cooling rates. We conclude that photo-ionization by the ionizing background and heavy elements both need to be taken into account in order for the cooling rates to be correct to order of magnitude. Moreover, if the rates need to be known to better than a factor of a few, then departures of the relative abundances from solar need to be taken into account. We propose a method to compute cooling rates on an element-by-element basis by interpolating pre-computed tables that take photo-ionization into account. We provide such tables for a popular model of the evolving UV/X-ray background radiation, computed using the photo-ionization package CLOUDY.

Key words: atomic processes — plasmas — cooling flows — galaxies: formation — intergalactic medium

1 INTRODUCTION

Dissipation of energy via radiative cooling plays a central role in many different astrophysical contexts. In general the cooling rate depends on a large number of parameters, such as the gas density, temperature, chemical composition, ionization balance, and the radiation field. In the absence of radiation, however, the equilibrium ionization balance depends only on the temperature. In that case the cooling rate in the low density regime, which is dominated by collisional processes, is simply proportional to the gas density squared, for a given composition. Thus, the cooling rates for a plasma in collisional ionization equilibrium (CIE) can be conveniently tabulated as a function of the temperature and composition (metallicity) of the gas (e.g., Cox & Tucker 1969; Raymond et al. 1976; Shull & van Steenberg 1982; Gaetz & Salpeter 1983; Boehringer & Hensler 1989; Sutherland & Dopita 1993; Landi & Landini 1999; Benjamin et al. 2001; Gnat & Sternberg 2007; Smith et al. 2008), and such tables are widely used for a large variety of problems.

Although it is convenient to ignore radiation when calculating cooling rates, radiation is generally important for the thermal and ionization state of astrophysical plasmas. For example, Efstathiou (1992) investigated the effect of the extragalactic UV background on the cooling rates for gas of primordial composition (in practice this means a pure H/He plasma) and found that including photo-ionization can suppress the cooling rates of gas in the temperature range $T \sim 10^4 - 10^5\,\mathrm{K}$ by a large factor. Although the effects of radiation are often taken into account for gas of primordial composition, photo-ionization of heavy elements is usually ignored in the calculation of cooling rates (but see Leonard 1998; Benson et al. 2002).

⋆ E-mail: wiersma@strw.leidenuniv.nl

In this paper we will investigate the dependence of cooling rates of gas enriched with metals on the presence of ionizing radiation, focusing on the temperature range $T \sim 10^4 - 10^8\,\mathrm{K}$ and optically thin plasmas. We will show that, as is the case for gas of primordial composition (Efstathiou 1992), photo-ionization can suppress the metallic cooling rates by a large factor. Moreover, the suppression of the cooling rate is significant up to much higher temperatures than for the primordial case.

We will also investigate the relative contributions of various elements to the cooling rates. If the relative abundances are similar to solar, then oxygen, neon, and iron dominate the cooling in the temperature range $T \sim 10^4 - 10^7\,\mathrm{K}$. However, we will show that the relative contributions of different elements to the cooling rate are sensitive to the presence of ionizing radiation.

Although we will illustrate the results using densities and radiation fields that are relevant for studies of galaxy formation and the intergalactic medium (IGM), the conclusion that photo-ionization significantly reduces the cooling rates of enriched gas is valid for a large variety of astrophysical problems. For example, for $T \sim 10^5\,\mathrm{K}$ and $T \sim 10^6\,\mathrm{K}$ the reduction of metal-line cooling rates is significant as long as the dimensionless ionization parameter[1] $U \gtrsim 10^{-3}$ and $U \gtrsim 10^{-1}$, respectively. We will focus on the temperature range $10^4 - 10^8\,\mathrm{K}$ because gas in this temperature range is usually optically thin and because the effects of photo-ionization are generally unimportant at higher temperatures.

Tables containing cooling rates and several other useful quantities as a function of density, temperature, redshift, and composition, appropriate for gas exposed to the models for the evolving meta-galactic UV/X-ray background of Haardt & Madau (2001) are available on the following web site: `http://www.strw.leidenuniv.nl/WSS08/`. The web site also contains a number of videos that illustrate the dependence of the cooling rates on various parameters.

This paper is organized as follows. In Section 2 we present our method for calculating element-by-element cooling rates including photo-ionization and we compare the limiting case of CIE to results taken from the literature. Section 3 shows how metals and ionizing radiation affect the cooling rates. Section 4 demonstrates the importance for the low-redshift shock-heated IGM, which is thought to contain most of the baryons. In this section we also illustrate the effect of changing the intensity and spectral shape of the ionizing radiation. We investigate the effect of photo-ionization on the relative contributions of individual elements in Section 5 and we summarize and discuss our conclusions in Section 6.

Throughout this paper we use the cosmological parameters from Komatsu et al. (2008): $(\Omega_\mathrm{m}, \Omega_\Lambda, \Omega_\mathrm{b}, h) = (0.279, 0.721, 0.0462, 0.701)$ and a primordial helium mass fraction $X_\mathrm{He} = 0.248$. Densities will be expressed both as proper hydrogen number densities n_H and density contrasts $\delta \equiv \rho_\mathrm{b}/\langle\rho_\mathrm{b}\rangle - 1$, where $\langle\rho_\mathrm{b}\rangle$ is the cosmic mean baryon density. The two are related by

$$n_\mathrm{H} \approx 1.9 \times 10^{-7}\,\mathrm{cm}^{-3}\ (1+\delta)\,(1+z)^3 \left(\frac{X_\mathrm{H}}{0.752}\right). \quad (1)$$

[1] $U \equiv \Phi_\mathrm{H}/(n_\mathrm{H} c)$, where Φ_H is the flux of hydrogen ionizing photons (i.e., photons per unit area and time), n_H is the total hydrogen number density and c is the speed of light.

Table 1. Default CLOUDY solar abundances

Element	n_i/n_H	Mass Fraction
H	1	0.7065
He	0.1	0.2806
C	2.46×10^{-4}	2.07×10^{-3}
N	8.51×10^{-5}	8.36×10^{-4}
O	4.90×10^{-4}	5.49×10^{-3}
Ne	1.00×10^{-4}	1.41×10^{-3}
Mg	3.47×10^{-5}	5.91×10^{-4}
Si	3.47×10^{-5}	6.83×10^{-4}
S	1.86×10^{-5}	4.09×10^{-4}
Ca	2.29×10^{-6}	6.44×10^{-5}
Fe	2.82×10^{-5}	1.10×10^{-3}

2 METHOD

All radiative cooling and heating rates were computed by running large grids of photo-ionization models using the publicly available photo-ionization package CLOUDY[2] (version 07.02 of the code last described by Ferland et al. 1998). CLOUDY contains most of the atomic processes that are thought to be important in the temperature range of interest here ($T \sim 10^4 - 10^8\,\mathrm{K}$) and the reader is referred to the online documentation for details about the atomic physics and data used.

The gas was exposed to the cosmic microwave background radiation (CMB) and the Haardt & Madau (2001, hereafter HM01) model[3] for the UV/X-ray background radiation from galaxies (assuming a 10 percent escape fraction for H-ionizing photons) and quasars. We assumed the gas to be dust-free, optically thin and in ionization equilibrium. We discuss the limitations and the effects of the last two assumptions in section 6. All cooling rates are tabulated as a function of $\log n_\mathrm{H}$ (total hydrogen number density), $\log T$ (temperature), and z (redshift).

When studying the effect of changes in the relative abundances of elements, we compute the cooling rates on an element-by-element basis. The cooling rate Λ_i (in $\mathrm{erg\,s^{-1}\,cm^{-3}}$) due to element i, where element i is heavier than helium, is defined as the difference between the cooling rate computed using all elements (assuming solar abundances) and the cooling rate computed after setting the abundance of element i to zero, while keeping all other abundances (i.e., number densities relative to H) the same. This is a valid approximation provided element i does not contribute significantly to the free electron density, which is the case for all elements heavier than helium and if the metallicity $Z \lesssim Z_\odot$.

The combined contributions from hydrogen and helium are computed by interpolating in the four dimensions $\log n_\mathrm{H}$, $\log T$, z, and $n_\mathrm{He}/n_\mathrm{H}$ from tables of CLOUDY models that contain only H and He.

Thus, the total net cooling rate,

[2] `http://www.nublado.org/`

[3] `http://pitto.mib.infn.it/~haardt/refmodel.html`

$$\Lambda = \Lambda_{\rm H,He} + \sum_{i>{\rm He}} \Lambda_i, \tag{2}$$

could be obtained from

$$\Lambda = \Lambda_{\rm H,He} + \sum_{i>{\rm He}} \frac{n_i/n_{\rm H}}{(n_i/n_{\rm H})_\odot} \Lambda_{i,\odot}, \tag{3}$$

where $(n_i/n_{\rm H})_\odot$ is the solar abundance of element i (the default CLOUDY solar abundances are given in Table 1) and $\Lambda_{i,\odot}$ is the contribution of heavy element i to the radiative cooling rate for solar abundances, which we have tabulated as a function of $\log n_{\rm H}$, $\log T$, and z. Note that we use Λ to denote the cooling rate per unit volume ($\rm erg\,s^{-1}\,cm^{-3}$).

We can, however, do better than equation (3) by taking the dependence of the free electron density on He/H, into account (in equation (3), the electron density is implicitly assumed to be that corresponding to solar abundances - $n_{\rm He}/n_{\rm H} = 0.1$). Since cooling rates due to metals are dominated by collisions between ions and free electrons, Λ_i scales as the product of the free electron and ion densities, $\Lambda_i \propto n_{\rm e} n_i$. Hence,

$$\begin{aligned} \Lambda &= \Lambda_{\rm H,He} + \sum_{i>{\rm He}} \Lambda_{i,\odot} \left(\frac{n_{\rm e}}{n_{{\rm e},\odot}}\right) \left(\frac{n_i}{n_{i,\odot}}\right), \\ &= \Lambda_{\rm H,He} + \sum_{i>{\rm He}} \Lambda_{i,\odot} \frac{n_{\rm e}/n_{\rm H}}{(n_{\rm e}/n_{\rm H})_\odot} 10^{[i/{\rm H}]} \end{aligned} \tag{4}$$

where $10^{[i/{\rm H}]} \equiv (n_i/n_{\rm H})/(n_i/n_{\rm H})_\odot$ and we used the fact that $n_{\rm H} = n_{{\rm H},\odot}$ (since we tabulate as a function of $n_{\rm H}$). While $(n_{\rm e}/n_{\rm H})_\odot$ is obtained by interpolating the solar abundance table for $n_{\rm e}/n_{\rm H}$ in $(n_{\rm H}, T, z)$, $(n_{\rm e}/n_{\rm H})$ must be obtained by interpolating in $((n_{\rm He}/n_{\rm H}), n_{\rm H}, T, z)$. Note that we tabulate the electron density in the absence of metals. This is a valid approximation given that heavy elements only contribute significantly to the free electron density for $Z \gg Z_\odot$.

In practice we tabulate $\log \Lambda_{i,\odot}/n_{\rm H}^2$ over the range $\log[n_{\rm H}\,({\rm cm^{-3}})] = -8.0$, -7.9, ..., 0.0 and $\log[T\ ({\rm K})] = 2.00$, 2.02, ..., 9.00. In addition, the quantities $\log \Lambda_{\rm H,He}/n_{\rm H}^2$, $n_{\rm e}/n_{\rm H}$ and the mean particle mass are all tabulated as a function of density and temperature for each of the values $n_{\rm He}/n_{\rm H} = 0.0787$, 0.0830, 0.0876, 0.0922, 0.970, 0.102, 0.107 which correspond to mass fractions $X_{\rm He}/(X_{\rm H} + X_{\rm He}) = 0.238$, 0.248, 0.258, 0.268, 0.278, 0.288, 0.298. Finally, for each value of the ratio $n_{\rm He}/n_{\rm H}$ we tabulate the temperature as a function of density and internal energy per unit mass to enable simulation codes that parametrize thermal energy in terms of the latter quantity to use the cooling tables. We have computed these tables for each of the 49 redshifts spanning $z = 0 - 9$ for which the HM01 models are defined. All tables are in HDF5 format and together they result in upwards of 232 MB of storage. Reducing the resolution in $n_{\rm H}$ and T by a factor of two does reduce the accuracy of interpolated rates significantly[4], but reduces the storage requirements to 61 MB.

We find that for metallicities $Z \lesssim Z_\odot$ equation (4) closely matches the true cooling rate (i.e., including all elements) with very good accuracy[5] if the following 11 elements are included: H, He, C, N, O, Ne, Mg, Si, S, Ca, and Fe.

For redshift $z = 0$ and over the full range of densities and temperatures, the median relative errors in the absolute net cooling rates are 0.33%, 1.6%, and 6.1% for $Z = 0.1Z_\odot$, $Z_\odot$, and $10Z_\odot$, respectively (we have scaled $n_{\rm He}/n_{\rm H}$ with metallicity). For higher redshifts the median errors are smaller than for $z = 0$ because Compton cooling off the CMB, which is modelled accurately, becomes increasingly important. Hence, even for metallicities as extreme as 10 times solar, using equation (4) and including 11 elements gives errors of only a few percent. As we shall see below, this is much smaller than the differences between different photo-ionization codes. Using equation (3) rather than (4) gives similar errors for low metallicities, but the median errors are a factor 2–3 higher for $Z > 10^{0.5}\ Z_\odot$.

Excluding temperatures within 0.1 dex of the thermal equilibrium solution (where the relative errors in the net

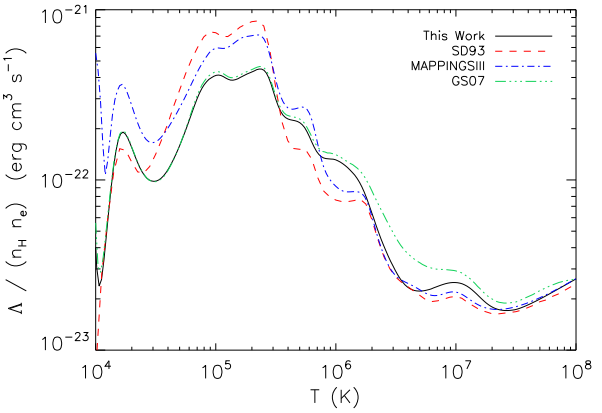

Figure 1. Comparison of normalized CIE cooling rates for various studies. All curves use the solar abundances of Gnat & Sternberg (2007), which differ somewhat from our default solar abundances. Shown are CLOUDY version 07.02 (solid), Sutherland & Dopita (1993) (dashed), MAPPINGS III (dot-dashed), and Gnat & Sternberg (2007) (dot-dot-dot-dashed). MAPPINGS gives significantly higher cooling rates for $T \sim 10^5$ K, but the differences are typically smaller than a factor of two. Note that for this comparison the cooling rates were divided by $n_{\rm H} n_{\rm e}$, but that we divide by $n_{\rm H}^2$ in our tables and in figure 6. The upturn in the normalized cooling rates below 10^4 K is caused by the sharp decrease in $n_{\rm e}$ with decreasing temperature.

[4] Reducing the temperature resolution by a factor of two roughly doubles the interpolation errors near the thermal equilibrium solution, but in this regime the cooling times are in any case effectively infinite.

[5] While the error in the total cooling rates is small, the relative errors in the contribution of individual elements can be larger if the element contributes negligibly to the total cooling rate (see e.g., the noise in the Fe contour at $T < 10^5$ K in the left-hand panel of figure 6). This is because the tables for individual elements were computed by taking the difference between the total cooling rate for solar abundances including and excluding the element. Hence, if the element does not contribute significantly to the cooling rate for a particular density, temperature, and redshift, then its contribution will be computed as the difference between two nearly equal numbers. Because this can only occur if the contribution is negligible, we do not consider this to be a problem.

cooling rate, which is computed as the absolute difference between heating and cooling, become large because we are subtracting two nearly identical numbers), the maximum errors in the net cooling rates are 32%, 29%, and 39% for $Z = 0.1Z_\odot$, $Z_\odot$, and $10Z_\odot$, respectively. Thus, even for extreme metallicities the maximum difference between the estimated and true rates is well within a factor of two. These maxima are reached near the 0.1 dex exclusion zone, so the maximum errors for temperatures that differ substantially from the equilibrium values are much smaller.

We have also tabulated the combined cooling rates of all elements heavier than helium, assuming solar relative abundances. While scaling all heavy elements simultaneously reduces the accuracy (relative to scaling the contribution of each element individually), these tables may be convenient in the absence of a complete set of elemental abundances. In this case, the total cooling rate becomes:

$$\Lambda = \Lambda_{\rm H,He} + \Lambda_{Z,\odot} \frac{n_{\rm e}/n_{\rm H}}{(n_{\rm e}/n_{\rm H})_\odot} \frac{Z}{Z_\odot}. \quad (5)$$

Although cooling rates including photo-ionization have not yet been tabulated, CIE cooling rates have been published by various authors. In Figure 1 we compare our CIE results (i.e., CLOUDY version 07.02) with those of Gnat & Sternberg (2007) (who used CLOUDY version 06.02), Sutherland & Dopita (1993) (who used MAPPINGS) and also with MAPPINGS III (version r; Groves et al. 2008). The calculations generally differ in terms of the code, the atomic rates, and the solar abundances that were used. In order to focus the comparison on codes and rates, we used the solar abundances assumed by Gnat & Sternberg (2007) when computing the cooling rates for all curves in this figure[6]. Note that these abundances differ somewhat from the solar abundances that we use in the rest of this paper.

The differences in the cooling rates shown in Figure 1 are typically smaller than 0.3 dex suggesting that the cooling rates are known to better than a factor of two, at least for CIE. The differences are largest for $T \sim 10^5$ K, with MAPPINGS giving higher cooling rates than CLOUDY.

3 PHOTO-IONIZATION, METALS, AND COOLING RATES

The cooling rates in photo-ionization equilibrium are not proportional to the density squared, as is the case for CIE. As a consequence, the cooling curve changes dramatically with density. This is illustrated in Fig. 2 which shows normalized, net cooling, rates ($|\Lambda/n_{\rm H}^2|$), as a function of temperature for solar abundances. Different curves correspond to different densities, as indicated in the legend.

The calculation includes the CMB and the HM01 background at redshift three. The $z = 3$ HM01 background corresponds to a hydrogen photo-ionization rate $\Gamma_{12} \equiv \Gamma/10^{-12}$ s^{-1} $= 1.1$ and an ionization parameter $U = 1.6 \times 10^{-5}/n_{\rm H}$. We stress that in the vicinity of ionizing sources the radiation field may be much more intense, which would enhance its effect on the cooling rates compared to the results presented here.

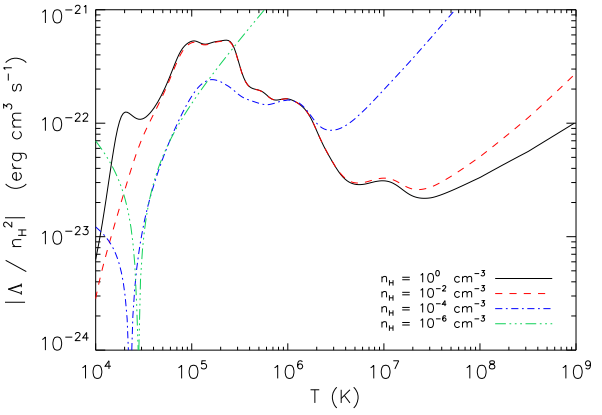

Figure 2. Normalized, absolute, net cooling rates ($|\Lambda/n_{\rm H}^2|$) as a function of temperature for solar abundances. Different curves correspond to different gas densities, as indicated in the legend. The gas in all models is exposed to the $z = 3$ CMB and the $z = 3$ HM01 UV/X-ray background. Note that the cooling rates were divided by $n_{\rm H}^2$, but that we divided by $n_{\rm H}n_{\rm e}$ in Fig. 1.

As the density decreases the gas becomes more highly ionized and the cooling peaks due to collisional excitation of various ions disappear. For very low densities and high temperatures the normalized cooling rates actually increase as they become dominated by Compton cooling off the CMB, which scales as $\Lambda \propto n_{\rm e}T$. For the two lowest densities shown, the equilibrium temperature, for which the net cooling rate $\Lambda \to 0$, exceeds 10^4 K. In these cases, curves corresponding to net heating appear to the left of the thermal equilibrium temperature.

Figure 3 shows how the presence of heavy elements and radiation affects the radiative cooling time. Each panel shows contours of constant cooling time in the density-temperature plane for two models. The top panels illustrate well known results, while the bottom panels demonstrate the importance of radiation on the cooling due to metal lines.

Here and throughout the cooling time refers to the absolute value of the net radiative cooling time at a fixed hydrogen density,

$$t_{\rm cool} \equiv \frac{T}{dT/dt} = \frac{\frac{3}{2}nkT}{|\Lambda_{\rm heat} - \Lambda_{\rm cool}|}. \quad (6)$$

For temperatures below the thermal equilibrium temperature, $t_{\rm cool}$ corresponds to a heating timescale. The calculation includes the CMB and, optionally, the HM01 background at redshift three.

Note that adiabatic cooling due to the expansion of the Universe is not included, but would dominate over radiative cooling for sufficiently low densities. For example, the universal Hubble expansion (appropriate for densities around the cosmic mean, i.e., $n_{\rm H} \sim 10^{-5}\,{\rm cm}^{-3}$ at $z = 3$) corresponds to an adiabatic cooling time $t_{\rm cool,adiab} = 1/(2H) \approx 1.6 \times 10^9$ yr at $z = 3$.

The top-left panel shows that for a metal-free[7] gas,

[6] Sutherland & Dopita (1993) only give the cooling rates as a function of the abundance of iron, which we interpolated to the corresponding Gnat & Sternberg (2007) value.

[7] We use $n_{\rm He}/n_{\rm H} = 0.083$ for primordial abundances.

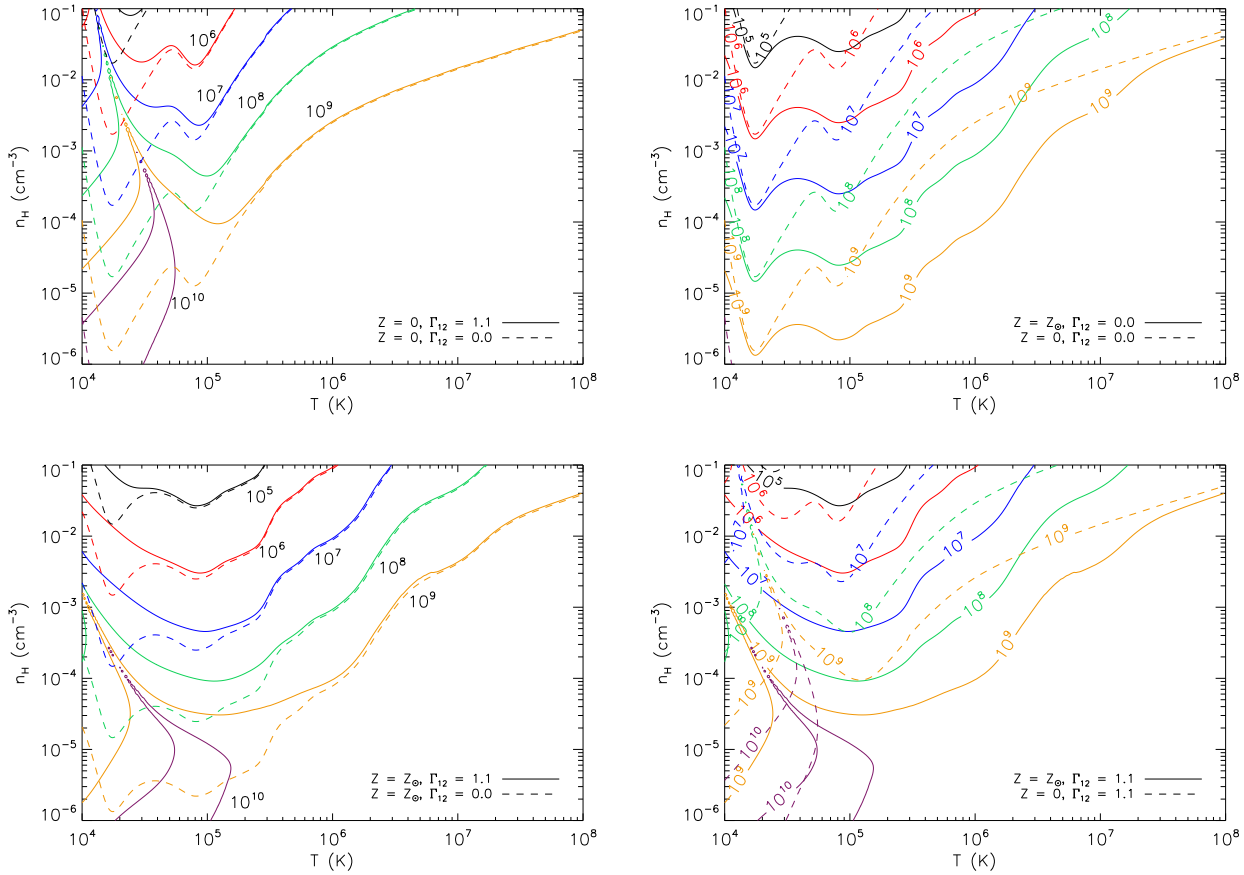

Figure 3. Contour plots of the net cooling time in years as a function of temperature and total hydrogen number density (note that the mean baryon density corresponds to $n_{\rm H} \sim 10^{-5}\,{\rm cm}^{-3}$ at $z = 3$). For temperatures below the equilibrium temperature, the contours indicate negative net cooling times, that is, heating times (see text). The gas in all models is exposed to the $z = 3$ CMB. In addition, models for which the legend indicates $\Gamma_{12} = 1.1$ use the $z = 3$ HM01 UV/X-ray background. The figure confirms that both metals and photo-ionization affect the cooling rates significantly, and shows their combined effect. *Top-left:* The effect of photo-ionization for zero metallicity; *Top-right:* The effect of metallicity for a purely collisionally ionized plasma; *Bottom-left:* The effect of photo-ionization for solar metallicity; *Bottom-right:* The effect of metallicity for a photo-ionized plasma.

ionizing radiation drastically reduces the cooling rates for $10^4\,{\rm K} < T \lesssim 10^5{\rm K}$ (Efstathiou 1992). This happens because the peaks in the cooling rate due to collisional excitation of neutral hydrogen and singly ionized helium (followed by Lyα emission) are removed when the gas is photo-ionized.

In the presence of ionizing radiation (solid curves) there are actually two contours for each net cooling time, corresponding to net heating (left of the thermal equilibrium asymptote) and net cooling (right of the equilibrium asymptote). These two contours nearly merge[8] near the (density-dependent) thermal equilibrium temperature, slightly above $10^4\,{\rm K}$, where the net cooling time goes to infinity. Below this temperature, the heating time is dictated by the photo-heating rate.

For $T \gg 10^5\,{\rm K}$ photo-ionization has no effect on a metal-free gas because the plasma is already fully ionized by collisional processes. In this regime the plasma cools predominantly via the emission of Bremsstrahlung and/or inverse Compton scattering of CMB photons. The latter process is the dominant cooling mechanism for most of the baryons at high redshift ($z > 7$). In the plot inverse Compton cooling off the CMB dominates the radiative cooling rate at low densities and high temperatures, but the corresponding cooling time exceeds the Hubble time.

For diffuse, intergalactic gas (i.e., for density contrasts $\delta \ll 10^2$, corresponding to $n_{\rm H} \ll 10^{-3}\,{\rm cm}^{-3}$ at $z = 3$, much lower than expected in virialized objects, e.g., Coles & Lucchin 2002) of primordial composition, radiation increases the cooling time at $10^5\,{\rm K}$ by at least an order of magnitude and by much more at lower temperatures. Since the cooling times in this regime are comparable to the Hubble time, radiation will have a large effect on the fraction of the baryons that are hot. At densities corresponding to collapsed objects ($\delta \gtrsim 10^2$ or $n_{\rm H} \gtrsim 10^{-3}\,{\rm cm}^{-3}$ at $z = 3$), the increase in the cooling time is generally smaller, although it can still easily be an order of magnitude at temperatures as high as $10^{4.5}\,{\rm K}$.

The top-right panel shows that heavy elements strongly increase the cooling rate of a collisionally ionized plasma

[8] The fact that the contours really do merge and then disappear at high densities is due to the limitations of our plotting package and the finite resolution of our grid.

for $10^4\,\mathrm{K} \ll T \lesssim 10^7\,\mathrm{K}$ (e.g., Boehringer & Hensler 1989). Comparing the model with primordial abundances (dashed contours) to the one assuming solar metallicity (solid contours), we see that the cooling times typically differ by about an order of magnitude. The presence of metals allows radiative cooling through collisional excitation of a large number of ions at a variety of temperatures. For $T > 10^7\,\mathrm{K}$ the difference is smaller because there are few lines to excite since most elements are collisionally ionized to a very high degree. Bremsstrahlung is the dominant cooling mechanism at these very high temperatures.

The bottom-left panel demonstrates that ionizing radiation also strongly reduces the cooling rates when heavy elements dominate the cooling. This happens for the same reason as in the primordial case. The radiation field ionizes the plasma to a higher degree than it would be in CIE. Hence, the ions that are typically collisionally excited are not present, reducing the cooling rates.

Note that a similar thing happens when a collisionally ionized plasma is cooling more quickly than it can recombine. In that case the ionization balance shifts out of equilibrium leaving the gas too highly ionized for its temperature. As for photo-ionization, the associated reduction of the number of bound electrons with excitation energies low enough to be collisionally excited, reduces the cooling rate (e.g., Kafatos 1973; Shapiro & Moore 1976; Schmutzler & Tscharnuter 1993; Sutherland & Dopita 1993).

Comparing the models with (solid contours) and without ionizing radiation (dashed contours), we see that for densities characteristic of the diffuse IGM ($\delta \ll 10^2$ corresponding to $n_\mathrm{H} \ll 10^{-3}\,\mathrm{cm}^{-3}$ at $z = 3$), radiation significantly reduces the cooling rates for $T \lesssim 10^6\,\mathrm{K}$ and that the reduction typically exceeds one order of magnitude for $T \lesssim 3 \times 10^5\,\mathrm{K}$. For densities $n_\mathrm{H} \gtrsim 10^{-3}\,\mathrm{cm}^{-3}$ the cooling rates are only suppressed substantially for $T < 3 \times 10^4\,\mathrm{K}$. However, we stress that what matters here is the ionization parameter. Hence, a stronger radiation field will affect the cooling rates up to higher densities. Gas with a density characteristic of collapsed objects will typically be close to sources of ionizing radiation and may thus be exposed to a radiation field that is more intense than the meta-galactic UV background.

Finally, the bottom-right panel shows that metals strongly increase the cooling rates in the presence of an ionizing radiation field, as was the case for a collisionally ionized gas (top-right panel). For solar metallicity the cooling rate at $T < 10^7\,\mathrm{K}$ is typically an order of magnitude higher than for a primordial composition.

Note that for very low densities ($n_\mathrm{H} \lesssim 10^{-5}\,\mathrm{cm}^{-3}$) metals increase the equilibrium temperature (towards the left side of the region where the net cooling time is above 10^{10} years) because their presence boosts the photo-heating (via oxygen and iron[9]) but does not significantly affect the cooling because it is dominated by Compton cooling off the CMB.

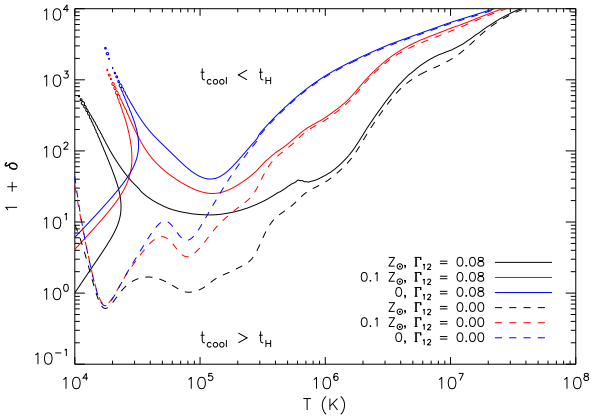

Figure 4. Contours show where the net cooling time equals the Hubble time in the density contrast - temperature plane at $z = 0$. From top to bottom, the different colours correspond to primordial composition (blue), a metallicity of ten percent solar (red), and solar abundances (black). Dashed contours are for collisional ionization only, while solid contours are for gas exposed to the HM01 model for the $z = 0$ UV/X-ray background. Each solid contour comprises two components, corresponding to net heating (low temperature component) and net cooling (high temperature component), respectively, which merge near the (density-dependent) thermal equilibrium temperature. Both photo-ionization and metallicity determine whether gas is able to cool and it is therefore crucial to take both into account when predicting the fraction of the baryons that reside in the WHIM.

4 EFFECT ON THE WHIM

The fraction of gas that has been shock-heated to temperatures of $10^5\,\mathrm{K} \lesssim T < 10^7\,\mathrm{K}$ is currently of great interest, mainly because this so-called warm-hot intergalactic medium (WHIM) is hard to detect, yet may contain a large fraction of the baryons in the low-redshift Universe (e.g., Cen & Ostriker 1999). There are two reasons why the WHIM becomes more important at lower redshift. First, as structure formation progresses, larger structures form, leading to stronger gravitational accretion shocks and a greater fraction of the baryons are heated to temperatures in the WHIM range. Second, as the universe expands, the density of the diffuse gas decreases as[10] $(1+z)^3$ and the cooling time due to collisional processes (which dominate for $z < 7$) will thus increase as $(1+z)^{-3}$. Hence, the cooling time increases faster than the Hubble time and more and more of the shock-heated gas is unable to cool.

Since the cooling times are of order the Hubble time for much of the WHIM, the precise values of the cooling rate is particularly important. Because the cooling of the WHIM tends to be dominated by line radiation, because its density is low ($\delta \sim 10 - 10^2$; e.g., Bertone et al. 2008), and because the WHIM gas may well be enriched to values of 10% of solar or higher, both metals and photo-ionization by the UV background may be important. Figure 4 demonstrates that this is indeed the case.

Figure 4 shows a contour plot of the cooling time in the

[9] The increased He/H ratio also boosts the photo-heating rate, but its contribution is smaller than that of the metals.

[10] In reality the density will decrease slightly less fast with time if the gas is overdense and collapsing.

density contrast-temperature plane for redshift $z = 0$. Each contour corresponds to the same net cooling time, namely the Hubble time. Dashed contours are for a purely collisionally ionized gas, while the solid contours include photo-ionization by the $z = 0$ UV/X-ray background radiation from galaxies and quasars, which corresponds to a hydrogen photo-ionization rate $\Gamma_{12} = 0.08$ and an ionization parameter $U = 9 \times 10^{-7}/n_{\rm H}$. Metallicity increases from the top down from zero (i.e., primordial abundances) (blue contours), to 10% solar (red) to solar (black), as indicated in the figure. Gas above a given contour is able to cool, while gas below it will remain hot.

For a primordial composition (blue contours), turning on the ionizing radiation raises the density contrast above which the gas can cool from $\delta \lesssim 10$ to $\delta \sim 10^2$ for $T < 10^5$ K. For solar metallicity, the UV radiation becomes important for $T < 10^6$ K and raises the critical density required for cooling within a Hubble time by about an order of magnitude for $T \lesssim 10^5$ K. Increasing the metallicity from zero to solar decreases the critical density contrast by about an order of magnitude over the full range of WHIM temperatures. Clearly, both photo-ionization and metals are important for the thermal evolution of the WHIM.

Figure 5 shows how the intensity and the spectral shape of the ionizing radiation affect the results for solar abundances. The solid contour indicates the density contrasts and temperatures for which the cooling time equals the Hubble time for the $z = 0$ HM01 model for the UV/X-ray radiation from quasars and galaxies (model QG). It is identical to the black, solid contour in Figure 4. The dashed contour shows the $t_{\rm cool} = t_H$ contour after we have multiplied the entire HM01 radiation field by a factor of 10 (model 10∗QG). Increasing the intensity reduces the cooling rates, shifting the contour to higher densities.

The dot-dashed contour corresponds to the quasar only HM01 model (model Q), which we have rescaled such as to give the same hydrogen ionization rate as model QG. Since the average energy of H-ionizing photons is higher for model Q than for QG, the difference between the dot-dashed and solid contours reflects the effect of changing the spectral hardness. Comparing these two contours, we see that, at a fixed H ionization rate, harder spectra tend to inhibit the cooling more than softer spectra for temperatures above the equilibrium value (the $t_{\rm cool} = t_H$ contour moves to higher densities for harder spectra). This happens because collisional excitation of heavy ions involves electrons with higher ionization energies than hydrogen. The extra high energy photons will remove many of those electrons, thus reducing the cooling rates further. For temperatures below the equilibrium value, however, the net cooling time actually decreases (the lower-left of the left contour moves to lower densities for harder spectra) because the photo-heating rates are larger for harder spectra.

In summary, for densities and temperatures characteristic of the WHIM the nature of the ionizing radiation field as well as the metallicity of the gas may have a significant impact. Accurate cooling rates therefore require a correct treatment of the composition of the gas, the spectral hardness, and the radiation intensity. Simple models may result in a poor estimate of the amount of baryons in the WHIM phase.

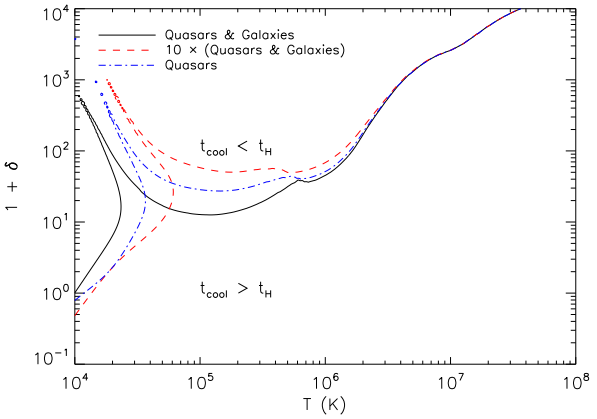

Figure 5. Contours show where the net cooling time equals the Hubble time in the density contrast - temperature plane for gas of solar metallicity at $z = 0$. The solid contour is for the HM01 model for the $z = 0$ UV/X-ray background from galaxies and quasars (model QG), the dashed contour is for a radiation field with the same spectral shape as model QG, but 10 times the intensity, and the dot-dashed contour is for the HM01 quasars only radiation field, scaled to the same hydrogen ionization rate as model QG. Each contour comprises two components, corresponding to net heating (low temperature component) and net cooling (high temperature component), respectively, which merge near the (density-dependent) thermal equilibrium temperature.

5 THE RELATIVE IMPORTANCE OF DIFFERENT ELEMENTS

For solar abundances, a large number of elements contribute to the radiative cooling rate. The black, solid curve in the left-hand panel of Figure 6 shows the normalized cooling rate ($\Lambda/n_{\rm H}^2$) as a function of temperature for a plasma in pure CIE and for solar abundances, reproducing previous work done on this subject (e.g., Cox & Tucker 1969; Raymond et al. 1976; Shull & van Steenberg 1982; Gaetz & Salpeter 1983; Boehringer & Hensler 1989; Sutherland & Dopita 1993; Landi & Landini 1999; Benjamin et al. 2001; Gnat & Sternberg 2007; Smith et al. 2008). The thin, coloured, solid curves show the contributions from individual elements, while the black, dashed curve shows the total cooling rate due to H and He. For $T \gg 10^7$ K Bremsstrahlung (i.e., H & He) dominates, but at lower temperatures line radiation is most important. Going down from 10^7 K to 10^4 K the cooling rate is successively dominated by iron, neon, oxygen, carbon, and hydrogen.

If the cooling rate is dominated by a single element, as is for example the case for oxygen at $T \approx 2\times10^5$ K and for iron at $T \sim 10^6$ K, then the total cooling rate will be sensitive to the relative abundances of those elements. For instance, since [O/Fe] is observed to vary with environment by factors of two or so at a fixed metallicity (e.g., Shetrone et al. 2003), we can expect similar variations in the cooling rates.

We next turn on the HM01 ionizing background and illustrate the results for $n_{\rm H} = 10^{-4}\,{\rm cm}^{-3}$ and $z = 3$ in the right-hand panel of Figure 6 (recall that the left-hand panel is independent of both density and redshift). For this figure we have excluded Compton cooling off the CMB to isolate the impact of the ionizing radiation and because the former

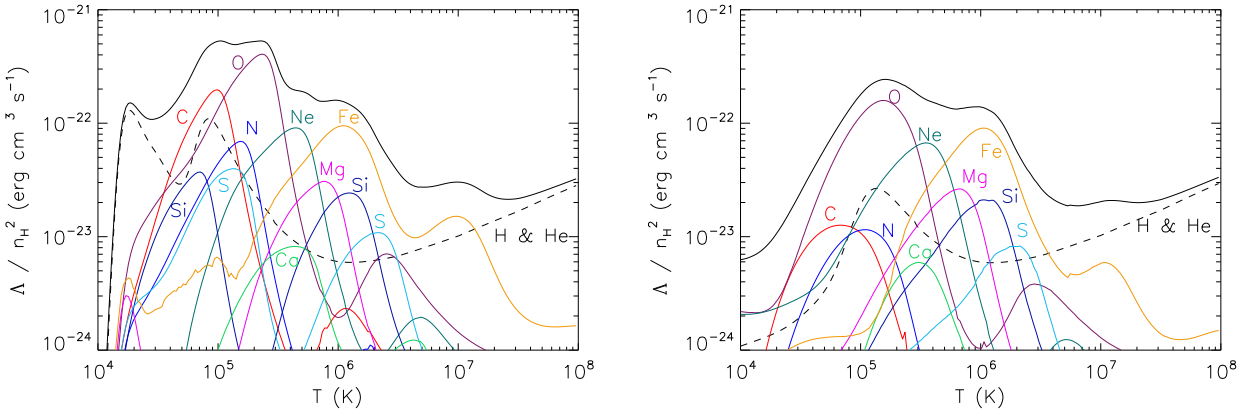

Figure 6. Normalized cooling rates as a function of temperature for solar abundances, assuming either CIE (*left-hand panel*) or photo-ionization equilibrium for $n_{\rm H} = 10^{-4}\,{\rm cm}^{-3}$ and an optically thin gas exposed to the $z = 3$ HM01 model for the meta-galactic UV/X-ray background from quasars and galaxies (*right-hand panel*). Note that normalized cooling rates are independent of the density for CIE, but not for photo-ionization equilibrium. The black, solid curve indicates the total cooling rate and the thin, coloured, solid curves show the contributions from individual elements. The black, dashed curve shows the contribution from H and He.

is only important at high redshift. We can see that photo-ionization affects some elements more than others. As we have seen before, the effect is stronger for lower temperatures. Although we show the results for only a single density here, we note that the importance of photo-ionization increases with decreasing density.

Comparing the cooling rates including photo-ionization (right-hand panel of figure 6) to those for CIE (left-hand panel of figure 6) shows that photo-ionization increases the relative importance of oxygen and decreases that of carbon, helium, and especially hydrogen. It is also clear that many of the peaks of the various elements shift to lower temperatures when an ionizing radiation field is present. This shift occurs because a photo-ionized gas is overionized for its temperature compared to a collisionally ionized plasma. If the ion fractions peak at lower temperatures, then so will the cooling rates due to collisional excitation of those ions.

This last figure illustrates the central result of this work: photo-ionization changes both the total cooling rates and the relative importance of individual elements. For a more complete visualization of this point, we kindly refer the interested reader to our web site[11], where we host a number of videos, plots, and the tables themselves for download.

6 DISCUSSION

Radiative cooling is an essential ingredient of hydrodynamical models of a wide range of astrophysical objects, ranging from the IGM to (proto-)galaxies and molecular clouds. While numerical simulations of objects with a primordial composition often compute non-equilibrium radiative cooling rates explicitly and sometimes even include the effect of ionizing background radiation, the treatment of cooling of chemically enriched material is typically much more approximate. For example, simulations of galaxy formation typically either ignore metal-line cooling altogether or include it assuming pure CIE. In addition, the abundances of all heavy elements are typically scaled by the same factor (the metallicity) (but see Martínez-Serrano et al. 2008 and Maio et al. 2007 for recent exceptions). In this simplified treatment metal-line cooling depends only on temperature and metallicity, allowing straightforward interpolation from pre-computed two-dimensional tables.

We have used CLOUDY to investigate the effects of heavy elements and ionizing radiation on the radiative cooling of gas with properties characteristic of (proto-)galaxies and the IGM, i.e., optically thin gas with densities $n_{\rm H} \lesssim 1\,{\rm cm}^{-3}$ and temperatures $T \gtrsim 10^4\,{\rm K}$, assuming ionization equilibrium. We presented a method to incorporate radiative cooling on an element-by-element basis including photo-ionization by an evolving UV/X-ray background, using precomputed tables, which for heavy elements are functions of density, temperature, and redshift and for H&He (which must be considered together because they are important contributors to the free electron density) depend additionally on the He/H ratio. Using the 11 elements H, He, C, N, O, Ne, Mg, Si, S, Ca, and Fe, the redshift $z = 0$ median absolute errors in the net cooling rate range from 0.33%, at $Z = 0.1Z_\odot$ to 6.1% for the extreme metallicity $Z = 10Z_\odot$, and the errors are smaller for higher redshifts.

The tables as well as some scripts that illustrate how to use them are available from the following web site: `http://www.strw.leidenuniv.nl/WSS08/`. We also include tables for solar relative abundances which can be used if metallicity, but not the abundances of individual elements are known, as in equation (5). This web site also contains a number of videos that may be helpful to gain intuition on the importance of various parameters on the cooling rates.

We confirmed that, assuming CIE, heavy elements greatly enhance the cooling rates for metallicities $Z \gtrsim 10^{-1}\,Z_\odot$ and temperatures $T \lesssim 10^7\,{\rm K}$. We demonstrated that this remains true in the presence of photo-ionization by the meta-galactic UV/X-ray background.

The background radiation removes electrons that would

[11] `http://www.strw.leidenuniv.nl/WSS08/`.

otherwise be collisionally excited, thus reducing the cooling rates. The effect is stronger for higher ionization parameters (i.e., higher radiation intensities or lower densities) and if the spectral shape of the radiation field is harder. Considering only the meta-galactic radiation field, which provides a lower limit to the intensity of the radiation to which optically thin gas may be exposed, the reduction of the metal-line cooling rates becomes important below 10^6 K for ionization parameters $U \gtrsim 10^{-1}$ and below 10^5 K for $U \gtrsim 10^{-3}$ (note that for the HM01 background $U = 9 \times 10^{-7}/n_{\rm H}$ and $2 \times 10^{-5}/n_{\rm H}$ at $z = 0$ and $z = 3$, respectively).

As an example of the potential importance of including the effects of both photo-ionization and heavy elements, we considered the so-called warm-hot intergalactic medium (WHIM), which is thought to contain a large fraction of the baryons at redshifts $z < 1$. We demonstrated that the overdensities for which gas at typical WHIM metallicities ($Z \sim 10^{-1}\ Z_\odot$) and temperatures ($T \sim 10^5 - 10^7$ K) can cool within a Hubble time, can shift by an order of magnitude depending on whether photo-ionization and metal-line cooling are taken into account. Hence, photo-ionization of heavy elements may have important consequences for predictions of the amount of matter contained in this elusive gas phase.

Because chemical enrichment happens in a number of stages, involving a number of processes with different timescales, the relative abundances of the heavy elements varies with redshift and environment by factors of a few. Hence, computing cooling rates on an element-by-element basis rather than scaling all elements by the metallicity, will change the cooling rates by factors of a few. The difference is therefore typically somewhat smaller than the effect of neglecting metals or photo-ionization altogether, but still highly significant.

While it was known that different elements dominate the cooling for different temperatures in CIE, we showed that photo-ionization both shifts the peaks due to individual elements to smaller temperatures and reduces their amplitude. Note that since photo-ionization over-ionizes the gas, this effect is similar (but not equivalent to) that found in non-equilibrium calculations without ionizing radiation (e.g., Sutherland & Dopita 1993; Gnat & Sternberg 2007). Because the importance of photo-ionization depends on the ionization parameter, the relative contributions of individual elements exposed to a fixed ionizing radiation field depends also on the gas density.

Would dropping our assumption of ionization equilibrium have a large effect on the cooling rates? Ionizing radiation results in a plasma that is overionized relative to its temperature. Its effect is therefore similar to that of non-equilibrium ionization following rapid cooling (i.e., if the cooling time is shorter than the recombination times of the ions dominating the cooling, see e.g., Kafatos 1973; Shapiro & Moore 1976). We therefore anticipate that the effect of non-equilibrium ionization will be much smaller for our cooling rates than for those that assume CIE.

The assumptions that the gas is optically thin and exposed only to the meta-galactic background radiation are likely to be more important than the assumption of ionization equilibrium, particularly since non-equilibrium collisional cooling rates only differ from those assuming CIE by factors of a few or less (e.g., Schmutzler & Tscharnuter 1993; Sutherland & Dopita 1993; Gnat & Sternberg 2007). For column densities $N_{\rm HI} > 10^{17}$ cm^{-2} self-shielding becomes important and only part of the H-ionizing radiation will penetrate the gas cloud, which would particularly affect the cooling rates for $T \lesssim 10^5$ K. At higher temperatures line cooling is dominated by heavier ions, which can only be ionized by higher energy photons and which therefore remain optically thin up to much higher column densities. This is because the photo-ionization cross sections of H and He drop rapidly with increasing frequency for energies exceeding their ionization potentials. Moreover, for $T \gg 10^4$ K hydrogen is collisionally ionized to a high degree and consequently the optical depth for ionizing radiation will be significantly reduced.

It is, however, far from clear that high column densities would reduce the effect of radiation. For self-shielded clouds the cooling radiation may itself be trapped, providing a source of ionizing radiation even in the absence of an external one (e.g., Shapiro & Moore 1976; Gnat & Sternberg 2007). Moreover, gas clouds with columns that exceed 10^{17} cm^{-2} are on average expected to be sufficiently close to a galaxy that local sources of ionizing radiation dominate over the background (Schaye 2006; Miralda-Escudé 2005).

Ultimately, these issues can only be resolved if non-equilibrium cooling rates are computed including radiative transfer and if the locations of all relevant sources of ionizing radiation are known. It will be some time before it is feasible to carry out such a calculation in, say, a cosmological hydrodynamical simulation. In the mean time, we believe that our element-by-element calculation of the equilibrium cooling rates for an optically thin gas exposed to the CMB and an evolving UV/X-ray background provides a marked improvement over earlier treatments. In future publications we will present cosmological, hydrodynamical simulations using these cooling rates.

ACKNOWLEDGMENTS

We are grateful to the anonymous referee whose helpful comments greatly improved the manuscript. We are also grateful to Gary Ferland for help with CLOUDY and to Brent Groves for help with MAPPINGS III. We would also like to thank Tom Abel and the members of the OWLS collaboration for discussions. In particular, we are grateful to Tom Theuns for showing us the benefits of HDF5. This work was supported by Marie Curie Excellence Grant MEXT-CT-2004-014112.

REFERENCES

Benjamin R. A., Benson B. A., Cox D. P., 2001, ApJ, 554, L225

Benson A. J., Lacey C. G., Baugh C. M., Cole S., Frenk C. S., 2002, MNRAS, 333, 156

Bertone S., Schaye J., Dolag K., 2008, Space Science Reviews, 134, 295

Boehringer H., Hensler G., 1989, A&A, 215, 147

Cen R., Ostriker J. P., 1999, ApJ, 514, 1

Coles P., Lucchin F., 2002, Cosmology: The Origin and Evolution of Cosmic Structure, Second Edition. Cosmology: The Origin and Evolution of Cosmic Struc-

ture, Second Edition, by Peter Coles, Francesco Lucchin, pp. 512. ISBN 0-471-48909-3. Wiley-VCH , July 2002.
Cox D. P., Tucker W. H., 1969, ApJ, 157, 1157
Efstathiou G., 1992, MNRAS, 256, 43P
Ferland G. J., Korista K. T., Verner D. A., Ferguson J. W., Kingdon J. B., Verner E. M., 1998, PASP, 110, 761
Gaetz T. J., Salpeter E. E., 1983, ApJS, 52, 155
Gnat O., Sternberg A., 2007, ApJS, 168, 213
Groves B., Dopita M. A., Sutherland R. S., Kewley L. J., Fischera J., Leitherer C., Brandl B., van Breugel W., 2008, ApJS, 176, 438
Haardt F., Madau P., 2001, in Neumann D. M., Tran J. T. V., eds, Clusters of Galaxies and the High Redshift Universe Observed in X-rays Modelling the UV/X-ray cosmic background with CUBA
Kafatos M., 1973, ApJ, 182, 433
Komatsu E., Dunkley J., Nolta M. R., Bennett C. L., Gold B., Hinshaw G., Jarosik N., Larson D., Limon M., Page L., Spergel D. N., Halpern M., Hill R. S., Kogut A., Meyer S. S., Tucker G. S., Weiland J. L., Wollack E., Wright E. L., 2008, ArXiv e-prints, 803
Landi E., Landini M., 1999, A&A, 347, 401
Leonard A., 1998, PhD thesis, University of Oxford
Maio U., Dolag K., Ciardi B., Tornatore L., 2007, MNRAS, 379, 963
Martínez-Serrano F. J., Serna A., Domínguez-Tenreiro R., Mollá M., 2008, ArXiv e-prints, 804
Miralda-Escudé J., 2005, ApJ, 620, L91
Raymond J. C., Cox D. P., Smith B. W., 1976, ApJ, 204, 290
Schaye J., 2006, ApJ, 643, 59
Schmutzler T., Tscharnuter W. M., 1993, A&A, 273, 318
Shapiro P. R., Moore R. T., 1976, ApJ, 207, 460
Shetrone M., Venn K. A., Tolstoy E., Primas F., Hill V., Kaufer A., 2003, AJ, 125, 684
Shull J. M., van Steenberg M., 1982, ApJS, 48, 95
Smith B., Sigurdsson S., Abel T., 2008, MNRAS, 385, 1443
Sutherland R. S., Dopita M. A., 1993, ApJS, 88, 253